

# Sensitivity of a Future High Energy $e^+e^-$ Collider to $Z'$ Bosons

David Kapukchyan and Tim M.P. Tait

*Department of Physics and Astronomy, University of California, Irvine, CA 92697, USA*

(Dated: April 29, 2022)

We consider the capability of a future high energy  $e^+e^-$  collider to search for the  $Z'$  bosons associated with a  $U(1)'$  gauge extension of the Standard Model. Even for  $Z'$  masses well above the center of mass energy of the collider, the rates of production of  $e^+e^-$ ,  $\mu^+\mu^-$ , unflavored jets, and  $b$ -tagged jets can reveal the presence of virtual  $Z'$  exchange. We consider collider configurations with center-of-mass energy 200, 300, and 500 GeV, and show how various classes of  $Z'$  model-lines can be probed with  $100 \text{ fb}^{-1}$  of integrated luminosity. We find that for order one couplings,  $Z'$  masses on the order of several TeV can be discovered, depending on the collider energy. Our results suggest that a 200 GeV collision energy is unlikely to discover any of the  $Z'$  models we consider that would not have already been visible in late stages of LHC running, but could still help refine understanding of the couplings and distinguish between different models. For  $e^+e^-$  collision energies of 300 GeV, parameter space beyond the reach of the LHC becomes accessible.

PACS numbers:

## I. INTRODUCTION

The Standard Model (SM) explains all the data from experiments so far, but many aspects of its underlying structure remain mysterious. As an immediate example, it is clear that local  $SU(3) \times SU(2) \times U(1)$  gauge invariance plays a huge role in its formulation, but it is not clear why Nature made this choice, as opposed to some other one. Given our lack of understanding, an obvious place to look for physics beyond the SM is by extending the gauge sector, and the simplest extension is an extra  $U(1)'$  group factor. In fact, such an addition to the SM is also motivated by theoretical considerations. The gauge structure of the SM and its fermionic matter content both fit preternaturally into an  $SU(5)$  grand unified theory (GUT). Larger groups such as  $SO(10)$  and  $E_6$ , motivated by UV completions of gravity, often contain remnant  $U(1)$ 's at low energies [1, 2].

The experimental hallmark of a  $U(1)'$  extension is the existence of an electrically neutral spin one boson – a  $Z'$ . Provided the  $Z'$  has couplings with SM quarks and leptons, it can be produced as a resonance at high energy hadron colliders [3]. Current searches for the reaction  $q\bar{q} \rightarrow Z' \rightarrow \ell^+\ell^-$  (where  $\ell = e$  or  $\mu$ ) at the LHC have provided powerful bounds on this kind of scenario, requiring the  $Z'$  mass to be larger than about 2.5 TeV, if it has order one couplings to the SM fermions [4, 5]. More weakly coupled  $Z'$ s remain viable even at somewhat smaller masses. Ultimately, a  $Z'$  with order one couplings to both quarks and leptons is expected to be discovered at a high luminosity  $\sqrt{s} = 14 \text{ TeV}$  LHC run provided  $M_{Z'}$  is less than about 4-5 TeV [6]. While a high luminosity LHC has excellent prospects to detect a  $Z'$ , the relatively limited number of viable channels would nonetheless leave many questions about its nature unresolved.

Lepton colliders offer an alternative perspective on  $Z'$  searches. A near-future  $e^+e^-$  collider is unlikely to reach LHC energies, but is expected to achieve an unprece-

dent precision that would allow it to be sensitive to virtual  $Z'$ s whose masses are far beyond the center-of-mass energy. In fact, bounds from LEP II remain interesting and relevant constraints on realistic  $Z'$  models even in the current LHC era [7, 8].

In this article, we examine the discovery potential of a future  $e^+e^-$  collider operating at  $\sim 500 \text{ GeV}$  collision energy to discover a  $Z'$ . Unlike earlier studies [9–15] we focus on a set of models which are somewhat orthogonal generalizations of the usual  $E_6$ -inspired  $Z'$  models [8], and focus on lower energy running options,  $\sqrt{s} = 200, 300$ , and  $500 \text{ GeV}$ . These energies, while low enough to perhaps exclude the possibility of studying exotic states directly, would nonetheless allow for precision studies of the newly discovered [16, 17] Higgs boson [15, 18, 19] and electroweak interactions of the top quark [15, 20].

## II. $Z'$ MODELS AND SIGNAL

A completely generic  $U(1)'$  model is described by a large number of parameters, including the mass, coupling, and width<sup>1</sup> of the  $Z'$ , as well as the couplings to the SM fermions and Higgs boson. We specialize to the case in which the  $Z'$  charges of the fermions are generation-independent, motivated by the desire to limit contributions to flavor-changing neutral currents at tree level [8]. The important couplings are thus those to the left-handed quark doublet ( $g_{qL}$ ), the right-handed up-type quarks ( $g_{uR}$ ) and down-type quarks ( $g_{dR}$ ), and to the lepton doublet ( $g_{lL}$ ) and charged singlet ( $g_{lR}$ ). We further avoid strong electroweak precision constraints by

<sup>1</sup> The width is an important parameter in searches for on-shell  $Z'$ s, such as at the LHC, but is largely irrelevant for off-shell searches such as are more typical at  $e^+e^-$  colliders.

choosing models for which the SM Higgs is uncharged, preventing  $Z$ - $Z'$  mixing at tree level. Four interesting model-lines belonging to this class, and for which gauge anomalies can be cancelled by vector-like (under the SM) fermions are defined in Ref. [8]:  $U(1)_{\text{universal}}$ ,  $U(1)_{B-xL}$ ,  $U(1)_{10+x5}$ , and  $U(1)_{d-xu}$ . Each of these model-lines is further characterized by a continuous real parameter  $x$  which parameterizes a freedom to choose the charges of the SM fermions under  $U(1)'$  while maintaining the properties outlined above. The  $E_6$  model points are contained as special values of  $x$  (for some of the model-lines) within this wider framework [8]. In addition, the gauge coupling, which multiplies the charge in each interaction, and the  $Z'$  mass are independent parameters. The charges of the models in terms of  $x$  are summarized in Table I.

Tables

$Z'$ Model	$U(1)_{\text{universal}}$	$U(1)_{B-xL}$	$U(1)_{10+x5}$	$U(1)_{d-xu}$
$g_{qL}$	$x$	$\frac{1}{3}$	$\frac{1}{3}$	0
$g_{uR}$	$x$	$\frac{1}{3}$	$-\frac{1}{3}$	$-\frac{x}{3}$
$g_{dR}$	$x$	$\frac{1}{3}$	$-\frac{x}{3}$	$\frac{1}{3}$
$g_{lL}$	$x$	$x$	$\frac{x}{3}$	$-\frac{1+x}{3}$
$g_{lR}$	$x$	$x$	$-\frac{1}{3}$	$\frac{x}{3}$

TABLE I: Summary of the fermion charges for the four  $Z'$  models considered, in terms of the continuous real parameter  $x$ .

The LHC limits suggest that a  $Z'$  strongly enough coupled to be discoverable at a future high energy  $e^+e^-$  facility must have a mass well above the collider energy. As a result, it contributes to scattering virtually, effectively acting as a higher dimensional interaction which interferes with the SM contributions mediated by the photon and  $Z$  boson. We examine the rate for  $e^+e^-$  annihilation into electrons, muons, jets containing bottom quarks, and unflavored jets of hadrons (initiated by  $u$ ,  $d$ ,  $s$ , or  $c$  quarks). We do not explicitly consider  $\tau$  production, which is sensitive to poorly understood  $\tau$ -tagging rates at future detectors, or top production, which requires a more complicated analysis to identify the top decay products. Both of these are worthwhile, but not likely to make up the bulk of a  $Z'$  signal for our benchmark model-lines.

The influence of the  $Z'$  on the rate of a given channel depends on how it interferes with the SM amplitudes, leading either to an increase or depression compared to the SM expectation. We simulate the leading order rate with Madgraph 5 [21], with the showering and hadronization performed by Pythia [22] and then simulate the detector response using PGS [23].

We examine three different center-of-mass energies for the  $e^+e^-$  collisions,  $\sqrt{s} = 200, 300$ , and 500 GeV and

a total data set of  $\mathcal{L} = 100 \text{ fb}^{-1}$  integrated luminosity. For each energy, we determine the expected number of events in each channel assuming the SM is correct, and that the uncertainty in this quantity is dominated by the statistical error<sup>2</sup>. We consider a given parameter point discoverable if it leads to a deviation of  $5\sigma$  in the expected rate. We draw contours in the plane of the  $Z'$  mass versus  $x$  for fixed  $U(1)'$  gauge coupling  $g = 1$ , delineating the regions of parameter space in which a  $Z'$  is observable. It is worth noting that for much of the parameter space considered here, a high luminosity LHC would presumably discover the  $Z'$  before a future high energy  $e^+e^-$  collider begins operation. We choose  $5\sigma$  as a case where the  $e^+e^-$  collider can definitively identify the presence of the  $Z'$  in a given channel and also measure the deviation in that channel to order 20%.

### III. RESULTS

We summarize our findings in a series of Figures for each  $Z'$  model, showing the bounds that can be placed on each model-line in the parameter space of the  $Z'$  mass and  $x$ , for each production channel individually, as well as the inclusive rate of all channels combined. In Figures 1-5, we show the bounds on  $U(1)_{\text{universal}}$ , where all fermions charges are equal to  $x$  (which may then itself be interpreted as the  $U(1)$  gauge coupling). The plots illustrate regions where a  $5\sigma$  deviation from the SM expected rate is realized, in the plane of the  $Z'$  mass and the coupling (equivalent to  $x$  for  $U(1)_{\text{universal}}$ ). We choose not to present results for  $Z'$  masses below 500 GeV, where on-shell production becomes possible, and the bounds depend sensitively on the  $Z'$  width.

For  $U(1)_{\text{universal}}$ , the strongest bounds at a given collider energy come from the electron channel, largely because of the fact that the  $Z'$  can contribute via both  $t$ -channel as well as  $s$ -channel Feynman diagrams. As a result, the inclusive and electron-specific bounds are similar. The results indicate that even at 200 GeV,  $Z'$  masses up to around 4 TeV can be discovered for order one couplings, with the difficult-to-discover region lying in the regime of small coupling and large mass. This parameter space is likely to have been already covered by the high energy LHC run [6, 27], but already at 300 GeV, the  $e^+e^-$  collider is expected to have a somewhat longer reach.

These trends continue to be evident in other types of  $Z'$  models.  $U(1)_{B-xL}$  is very similar to the model with universal couplings, except for  $x \rightarrow 0$  (where searches involving leptons in the initial or final states are hopeless). As shown in Figure 6, the coverage based on the electron final state is essentially the same as for  $U(1)_{\text{universal}}$ , and this limit continues to dominate the other channels for

<sup>2</sup> This was the case for the LEP II  $Z'$  analyses [7].

the same reasons. One different feature is the fact that the over-all sign of the  $Z'$  contribution to jet final states is controlled by the sign of the parameter  $x$ , leading to very different results (shown in Figures 7 and 8) for positive and negative  $x$  values. The differences in rates would be helpful in disentangling the nature of a  $Z'$  signal. Even in cases where one would expect the LHC to have made an initial discovery and measured  $|x|$ , the sign of  $x$  can be determined even with relatively modest  $e^+e^-$  collision energy.

The results for  $U(1)_{10+x5}$  illustrate a case where the couplings vary more widely with the parameter  $x$ . The  $e^+e^-$  final state, illustrated in Figure 9, continues to provide the over-all best limit for most values of  $x$ . The fact that the coupling to right-handed leptons is fixed, whereas the sign of the coupling to  $g_{lL}$  is determined by the sign of  $x$ ; introduces a noticeable asymmetry to the discoverable region, which becomes much more pronounced in the reach using untagged jets (Figure 10), and  $b$ -tagged jets (Figure 11). Once again, it is clear that valuable information about the pattern of couplings to various SM fermions can be inferred from a multi-channel analysis, giving clues as to the nature of a  $Z'$  signal if one is observed. This model also illustrates the utility of running at different energies, which changes the interplay between the  $Z'$  exchange amplitude squared compared with its interference with the Standard Model amplitudes. At low  $Z'$  masses, the two are comparable and regions of parameter space exist where, for example (in the  $e^+e^-$  final state), the collider configuration with  $\sqrt{s} = 200$  GeV can have a slightly improved reach compared to the 300 GeV configuration, owing to cancellations between the two terms.

Similar features are present in  $U(1)_{d-xu}$ , shown in Figures 12. The  $e^+e^-$  final state remains the single most effective channel, and there are regions of parameter space around  $x \simeq 2$  and  $Z'$  masses slightly above 500 GeV where the destructive interference at the 300 or 500 GeV collider configuration weakens discovery potential compared to the 200 GeV configuration.

#### IV. INTERPLAY WITH LHC

As noted above, even in cases where the LHC would be likely to discover a  $Z'$  before a future  $e^+e^-$  collider begins operation, the  $e^+e^-$  environment can contribute much to refine the understanding of the  $Z'$  model.

As an example, we consider the case of  $U(1)_{B-xL}$  with  $x = 1$  and  $M_{Z'} = 3.5$  TeV. Such a  $Z'$  would not have been discovered in the current LHC data set, but is likely to be visible through the reaction  $pp \rightarrow \ell^+\ell^-$  in high luminosity running at  $\sqrt{s} = 14$  TeV [6]. This observation would unambiguously establish the existence of a new resonance coupled to both quarks and leptons. However, even with high luminosity, the LHC is unlikely to be able to sift the decay into unflavored dijets from the large backgrounds [24], and for these parameters observation

of a decay into  $t\bar{t}$  is expected to be marginal [25, 26]. The LHC observation would provide a measurement of the  $Z'$  mass, but its width would be far below the experimental resolution, and thus only weakly bounded from above.

Even at  $\sqrt{s} = 200$  GeV and with  $100 \text{ fb}^{-1}$ , a future  $e^+e^-$  collider would do much to clarify the nature of such an LHC discovery. From Figures 6-8, we see that the expectation is that such a machine would observe only the  $e^+e^- \rightarrow e^+e^-$  channel, narrowing down the space of possible explanations to those where the coupling to leptons is roughly comparable to the coupling to quarks. Comparison with Figure 4 indicates that the model with universal couplings would be strongly disfavored by the lack of a signal in jets. In terms of an interpretation within the framework of  $U(1)_{B-xL}$ , such an observation would provide a measurement of  $0.9 \leq |x| \leq 1.1$ . In fact, because the  $e^+e^-$  collider's primary observable is through interference with the SM process, the rate also provides information about the relative signs of the couplings. For example, from Figure 8, we see that for  $x \simeq 1$ , no signal in  $b$ -flavored jets is expected to be visible, whereas for  $x \simeq -1$ , a signal should be strongly visible.

For this particular example, even a low energy  $e^+e^-$  collider is able to essentially reconstruct much of the structure of the  $Z'$  couplings through simple rate information. If polarized beams or forward-backward asymmetries are employed, one can further dissect the chiral structure of the couplings [27–29] (which in this example are vector-like).

#### V. CONCLUSIONS

We have examined the discovery potential of a future  $e^+e^-$  collider to infer the existence of a  $Z'$  based on its virtual influence over the rate of SM fermions production, looking at four well-motivated  $Z'$  model-lines. We find that even at very modest energies of  $\sqrt{s} \simeq 300$  GeV, the discovery potential is somewhat higher than for the LHC at design energy, and valuable information about the nature of the  $Z'$  couplings can be inferred even for models that the LHC is expected to have already discovered. We have confined our discussion to the simplest rate-based observables; angular variables and polarized beams can extract even more information [27–29]. We leave such refinements for future work.

A future  $e^+e^-$  facility has the potential to transform our understanding of the Higgs boson. In this work, we see that it also has interesting potential to search for physics beyond the Standard Model.

#### Acknowledgments

The research of T.M.P.T. is supported in part by NSF grants PHY-0970171 and PHY-1316792 and by the University of California, Irvine through a Chancellor's fellowship.

- [1] P. Langacker, Phys. Rept. **72**, 185 (1981).  
 [2] J. L. Hewett and T. G. Rizzo, Phys. Rept. **183**, 193 (1989).  
 [3] A. Leike, Phys. Rept. **317**, 143 (1999) [hep-ph/9805494].  
 [4] [ATLAS Collaboration], ATLAS-CONF-2013-017.  
 [5] CMS Collaboration [CMS Collaboration], CMS-PAS-EXO-12-061.  
 [6] S. Godfrey and T. Martin, arXiv:1309.1688 [hep-ph].  
 [7] t. S. Electroweak [LEP and ALEPH and DELPHI and L3 and OPAL and LEP Electroweak Working Group and SLD Electroweak Group and SLD Heavy Flavor Group Collaborations], hep-ex/0312023.  
 [8] M. S. Carena, A. Daleo, B. A. Dobrescu and T. M. P. Tait, Phys. Rev. D **70**, 093009 (2004) [hep-ph/0408098].  
 [9] T. G. Rizzo, Phys. Rev. D **55**, 5483 (1997) [hep-ph/9612304].  
 [10] T. G. Rizzo, Phys. Rev. D **59**, 113004 (1999) [hep-ph/9811440].  
 [11] T. G. Rizzo, JHEP **0306**, 021 (2003) [hep-ph/0305077].  
 [12] A. Freitas, Phys. Rev. D **70**, 015008 (2004) [hep-ph/0403288].  
 [13] L. Basso, A. Belyaev, S. Moretti and G. M. Pruna, JHEP **0910** (2009) 006 [arXiv:0903.4777 [hep-ph]].  
 [14] J. -J. Blaising and J. D. Wells, arXiv:1208.1148 [hep-ph].  
 [15] H. Baer, T. Barklow, K. Fujii, Y. Gao, A. Hoang, S. Kanemura, J. List and H. E. Logan *et al.*, arXiv:1306.6352 [hep-ph].  
 [16] G. Aad *et al.* [ATLAS Collaboration], Phys. Lett. B **716**, 1 (2012) [arXiv:1207.7214 [hep-ex]].  
 [17] S. Chatrchyan *et al.* [CMS Collaboration], Phys. Lett. B **716**, 30 (2012) [arXiv:1207.7235 [hep-ex]].  
 [18] M. E. Peskin, arXiv:1207.2516 [hep-ph].  
 [19] M. Klute, R. Lafaye, T. Plehn, M. Rauch and D. Zerwas, Europhys. Lett. **101**, 51001 (2013) [arXiv:1301.1322 [hep-ph]].  
 [20] P. Batra and T. M. P. Tait, Phys. Rev. D **74**, 054021 (2006) [hep-ph/0606068].  
 [21] J. Alwall, M. Herquet, F. Maltoni, O. Mattelaer and T. Stelzer, JHEP **1106**, 128 (2011) [arXiv:1106.0522 [hep-ph]].  
 [22] T. Sjostrand, S. Mrenna and P. Z. Skands, Comput. Phys. Commun. **178**, 852 (2008) [arXiv:0710.3820 [hep-ph]].  
 [23] <http://www.physics.ucdavis.edu/~conway/research/software/pgs/pgs4-general.htm>  
 [24] F. Yu, arXiv:1308.1077 [hep-ph].  
 [25] V. Barger, T. Han and D. G. E. Walker, Phys. Rev. Lett. **100**, 031801 (2008) [hep-ph/0612016].  
 [26] K. Agashe, H. Davoudiasl, S. Gopalakrishna, T. Han, G. -Y. Huang, G. Perez, Z. -G. Si and A. Soni, Phys. Rev. D **76**, 115015 (2007) [arXiv:0709.0007 [hep-ph]].  
 [27] P. Osland, A. A. Pankov and A. V. Tsytin, Eur. Phys. J. C **67**, 191 (2010) [arXiv:0912.2806 [hep-ph]].  
 [28] F. Petriello and S. Quackenbush, Phys. Rev. D **77**, 115004 (2008) [arXiv:0801.4389 [hep-ph]].  
 [29] Y. Li, F. Petriello and S. Quackenbush, Phys. Rev. D **80**, 055018 (2009) [arXiv:0906.4132 [hep-ph]].

## Figures

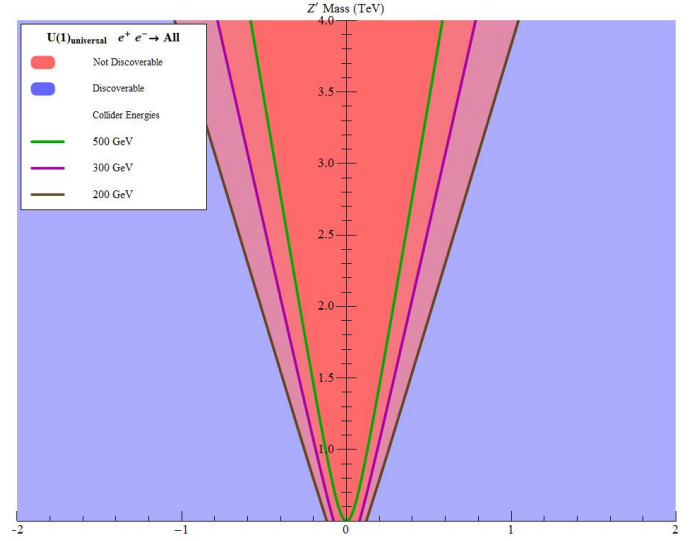


FIG. 1: The discoverable region of  $U(1)_{\text{universal}}$  for an  $e^+e^-$  collider running at 200, 300, or 500 GeV (as indicated) having collected  $100 \text{ fb}^{-1}$  of integrated luminosity, in the plane of the coupling and the  $Z'$  mass, based on the inclusive rate into SM fermions.

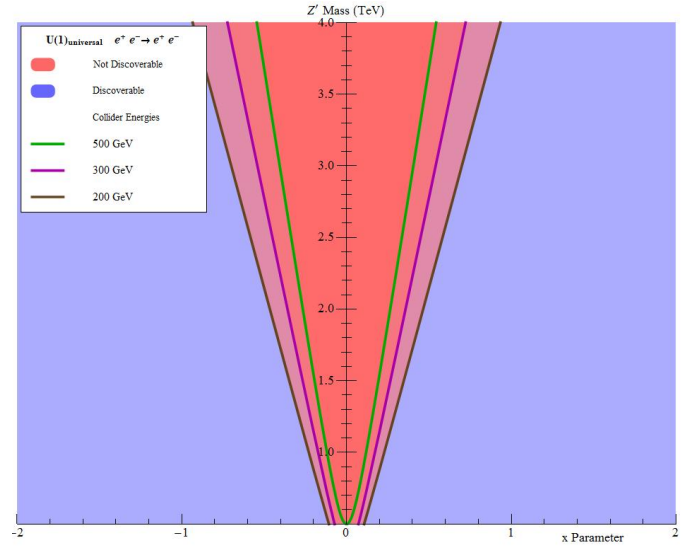


FIG. 2: Same as Figure 1, except for the exclusive  $e^+e^-$  final state.

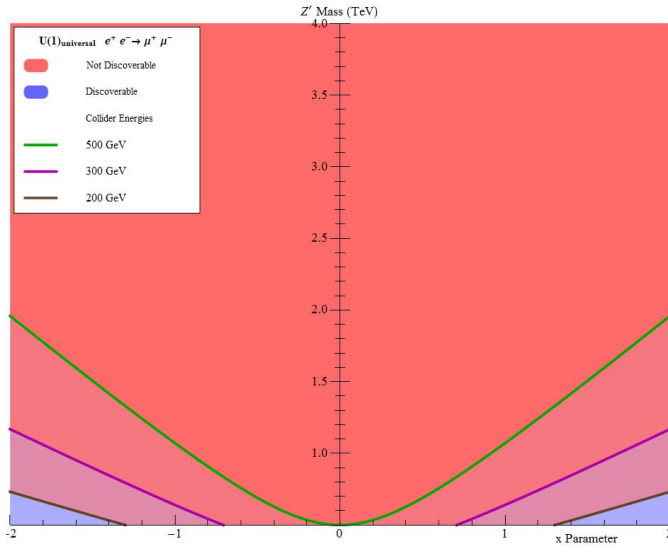


FIG. 3: Same as Figure 1, except for the exclusive  $\mu^+\mu^-$  final state.

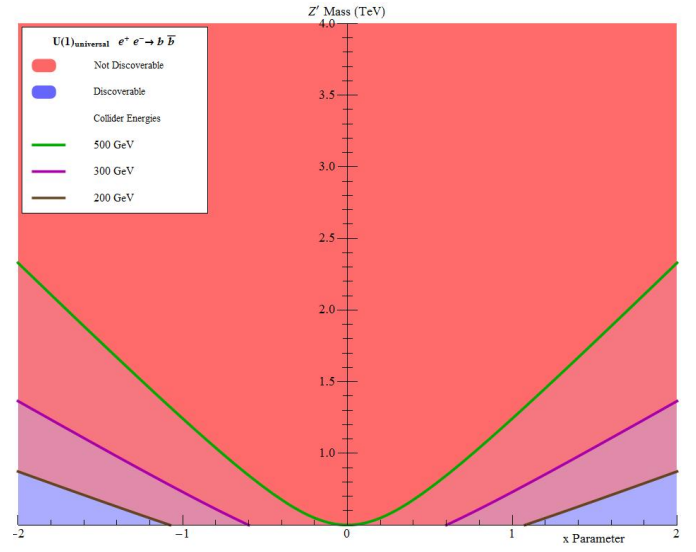


FIG. 5: Same as Figure 1, except for the exclusive  $b$ -jet final state.

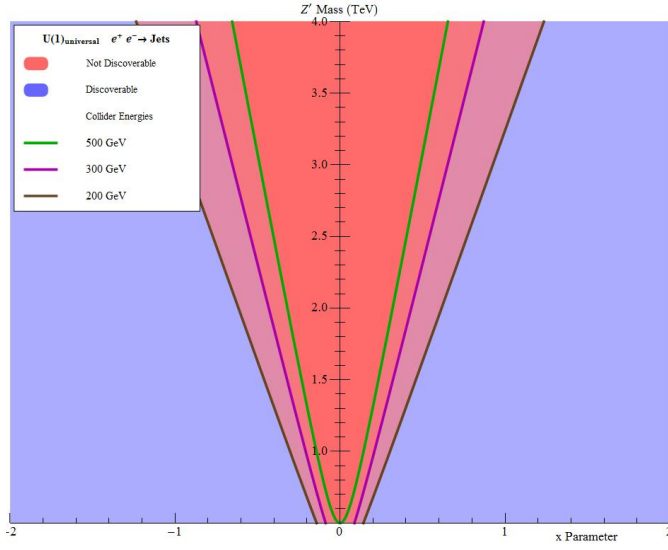


FIG. 4: Same as Figure 1, except for the exclusive unflavored jet final state.

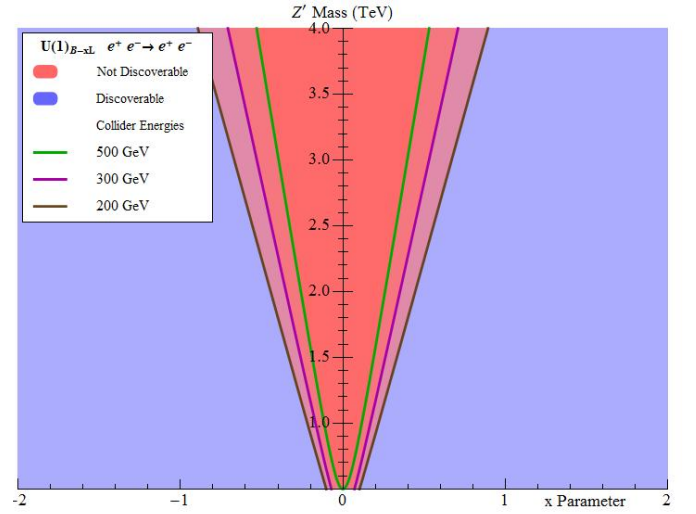


FIG. 6: The discoverable region of  $U(1)_{B-xL}$  for an  $e^+e^-$  collider running at 200, 300, or 500 GeV (as indicated) having collected  $100 \text{ fb}^{-1}$  of integrated luminosity, in the plane of the model parameter  $x$  and the  $Z'$  mass (for fixed gauge coupling  $g = 1$ ), based on the  $e^+e^-$  final state.

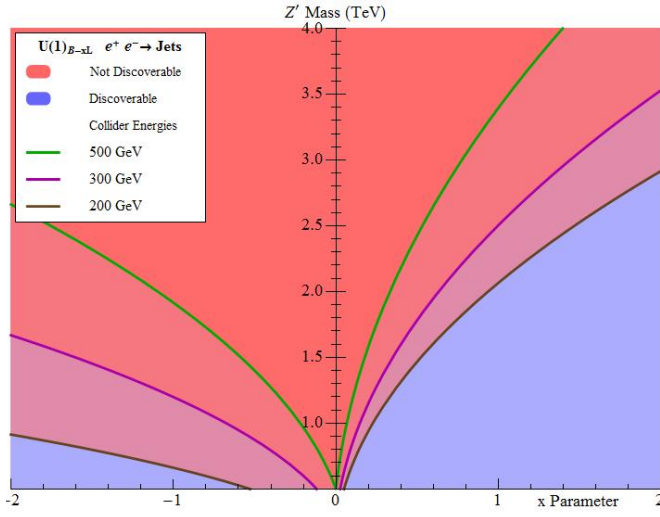


FIG. 7: Same as Figure 6, except for the exclusive unflavored jet final state.

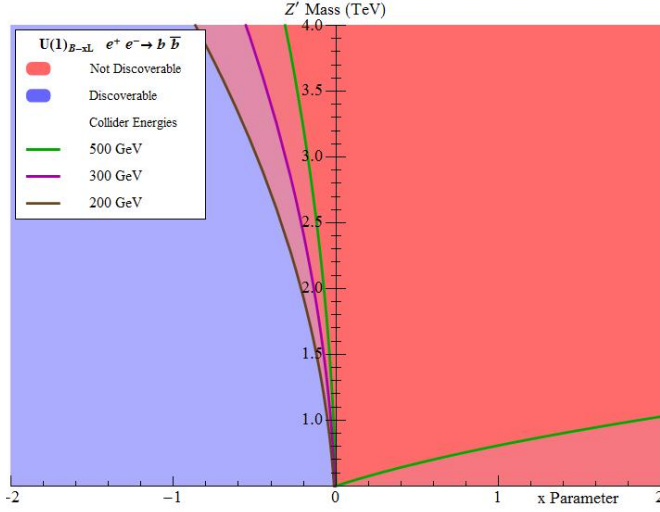


FIG. 8: Same as Figure 6, except for the exclusive  $b$ -jet final state.

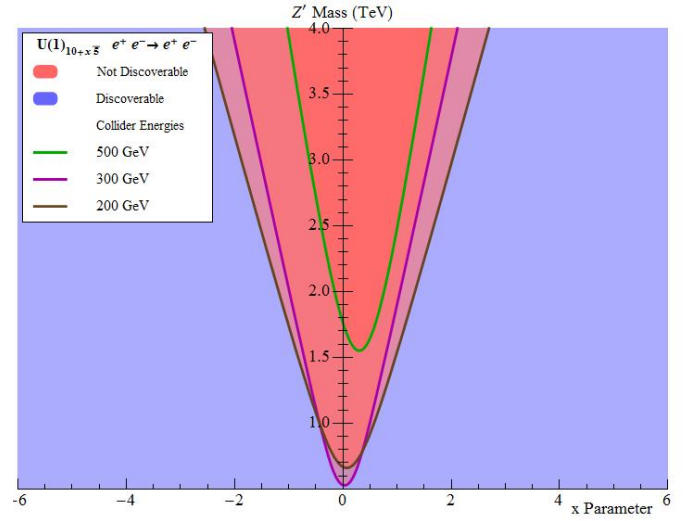


FIG. 9: The discoverable region of  $U(1)_{10+x5}$  for an  $e^+e^-$  collider running at 200, 300, or 500 GeV (as indicated) having collected  $100 \text{ fb}^{-1}$  of integrated luminosity, in the plane of the model parameter  $x$  and the  $Z'$  mass (for fixed gauge coupling  $g = 1$ ), based on the  $e^+e^-$  final state.

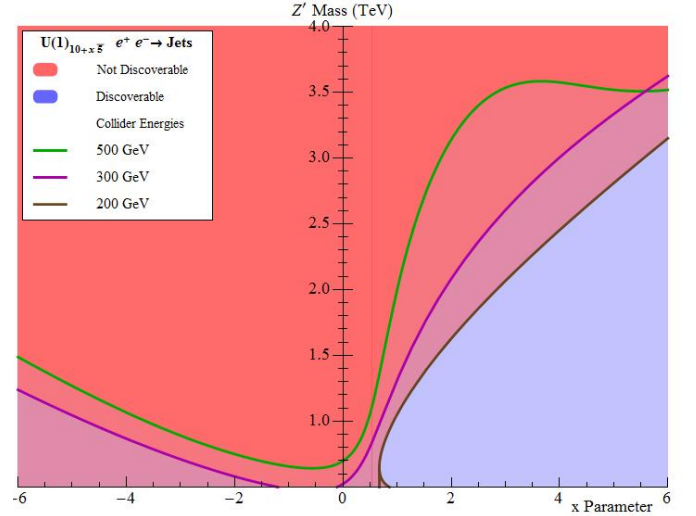


FIG. 10: Same as Figure 9, except for the exclusive unflavored jet final state.

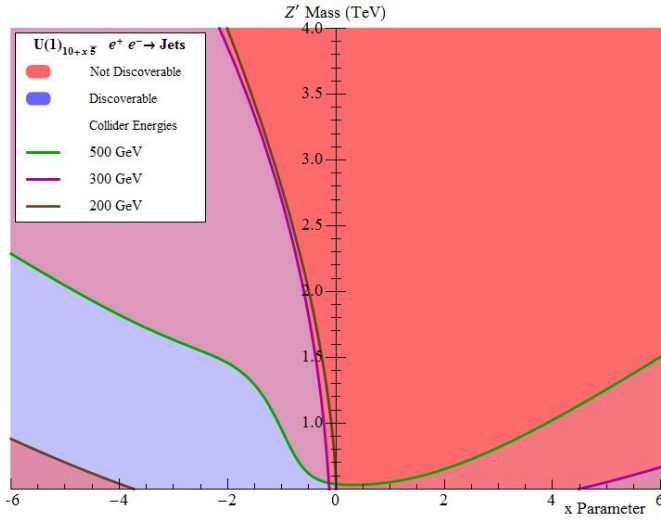


FIG. 11: Same as Figure 9, except for the exclusive  $b$ -jet final state.

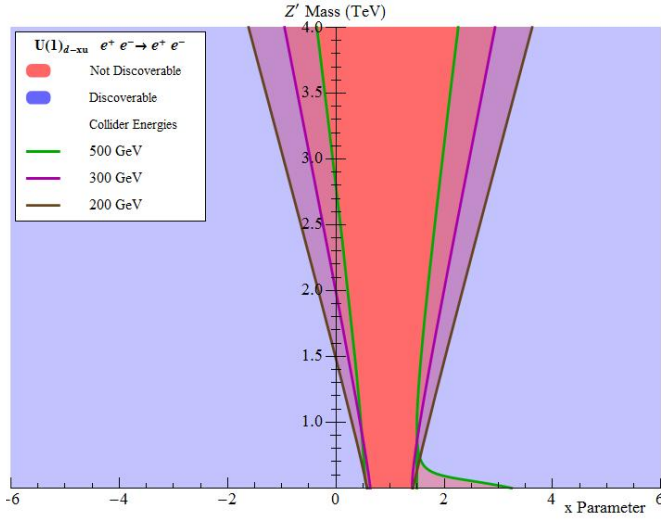


FIG. 12: The discoverable region of  $U(1)_{d-xu}$  for an  $e^+e^-$  collider running at 200, 300, or 500 GeV (as indicated) having collected  $100 \text{ fb}^{-1}$  of integrated luminosity, in the plane of the model parameter  $x$  and the  $Z'$  mass (for fixed gauge coupling  $g = 1$ ), based on the  $e^+e^-$  final state.